

# Linear Optical Sampling

C. Dorrer, D. C. Kilper, H. R. Stuart, G. Raybon, and M. G. Raymer

**Abstract**—We demonstrate the measurement of waveforms and eye diagrams at high bit rates by optical sampling using coherent detection. By simultaneously recording two orthogonal quadratures of the interference between the data stream and a sampling pulse with two balanced detectors, we are able to cancel the phase sensitivity inherent to linear optics. As the device is based on linear optics and square-law low-speed photodetectors, its sensitivity is 1000 times better than nonlinear optical sampling techniques, which makes it attractive for optical signal characterization and monitoring. This new diagnostic tool was used to measure eye diagrams at 10, 40, and 80 Gb/s, and is projected to operate at 160 Gb/s and higher.

**Index Terms**—Homodyne detection, interferometry, optical fiber communications, optical pulse measurements, sampling methods.

THE measurement of high-speed temporal waveforms is integral to the advancement of a range of technological fields, a prominent example being optical communications. While commercial communication systems have reached per-channel data rates of 40 Gb/s, data rates of 160 Gb/s and beyond are routinely generated in research laboratories today. Traditional optoelectronic measurement techniques, in which a high-speed photodetector and sample-and-hold circuit provide the temporal gating function, are presently inadequate at these ultrahigh data rates. One alternative is nonlinear optical sampling [1]–[5], which enables dramatically higher temporal resolution because a short optical pulse provides the gating function. This approach suffers from poor sensitivity because of the inherent low efficiency of nonlinear optical mixing. We present a new approach to optical waveform measurement, based on *linear* optical sampling. A short optical pulse provides the gating function and the sampling is accomplished using coherent homodyne mixing on a low-speed photodetector, a linear optical process. The phase sensitivity inherent to homodyne detection is removed by simultaneous measurement of orthogonal phase quadratures. This approach allows the characterization of nonperiodic waveforms (typically, a data-encoded train of pulses), for which phase-stepped or phase-averaged field cross-correlations cannot be used [6], [7]. We demonstrate eye diagram measurements with sensitivity three orders of magnitude better than previous optical techniques. The minimum input data signal peak power reported here is 60  $\mu$ W, compared with greater than 1 mW for other techniques. Compared to

optical sampling methods that measure average pulse shapes, such as two-photon absorption in silicon [8], [9], the sensitivity of linear sampling is still three orders of magnitude better. We first consider a single data pulse with field  $\varepsilon_D(t)$  and a single sampling pulse with field  $\varepsilon_S(t)$ . We assume that the two fields are copolarized. A delay  $\tau$  is introduced between the two pulses. If the two pulses are incident on a slow integrating photodetector, the output electrical current is

$$i_1 = B_S + B_D + 2\text{Re} \left[ \int \varepsilon_D(t) \varepsilon_S^*(t - \tau) dt \right] \quad (1)$$

where  $B_S$  and  $B_D$  are background terms proportional to the energy of the sampling pulse and the data pulse, respectively. Only the third term, the interferometric component, is of interest, as it carries information about the relative pulse shapes of the two pulses. The background can be a source of noise, for example, in case of fluctuations in the energy of the sampling pulses. In order to extract the interferometric component, we combine the two fields on a beam splitter and send each output to a separate detector in the conventional balanced homodyne configuration. The difference of the two photocurrents is

$$S_{12}(\tau) = i_1 - i_2 = 4\text{Re} \left[ \int \varepsilon_D(t) \varepsilon_S^*(t - \tau) dt \right]. \quad (2)$$

This signal directly depends on the phase of the temporal cross correlation between the two quickly varying fields and is, therefore, strongly phase dependent. Any change in the delay  $\tau$  by a fraction of the optical cycle (5 fs at 1550 nm) will modify  $S_{12}(\tau)$ . Phase locking the two sources would eliminate these problems, but this is too complex a solution for practical implementation. Phase averaging, i.e., the measurement of the root-mean-square value of  $S_{12}(\tau)$  when the phase between the two fields is stepped or randomized [6], [7], can be used only to measure the pulse shape averaged over many pulses. In order to measure the fluctuations on an optical signal, for example by constructing an eye diagram, each sampling event must be independently recorded without averaging.

To remove the phase dependence, we simultaneously measure both quadratures for each sampling event, i.e., the real and imaginary parts of the interferometric component. This is accomplished using two identical setups, and introducing a  $\pi/2$  phase shift between the fields in the second setup. In this case, the output of the balanced photodetector is

$$S_{34}(\tau) = 4\text{Im} \left[ \int \varepsilon_D(t) \varepsilon_S^*(t - \tau) dt \right]. \quad (3)$$

This quantity equals the other quadrature of the interferometric component. The two detected quadratures described by (2) and

Manuscript received March 5, 2003; revised June 19, 2003.

C. Dorrer, D. C. Kilper, and H. R. Stuart are with Bell Laboratories, Lucent Technologies, Holmdel, NJ 07733 USA (e-mail: dorrer@lucent.com).

G. Raybon is with Bell Laboratories, Lucent Technologies, Crawford Hill Laboratory, Holmdel, NJ 07733 USA.

M. G. Raymer is with the Department of Physics and Oregon Center for Optics, University of Oregon, Eugene, OR 97403 USA.

Digital Object Identifier 10.1109/LPT.2003.819729

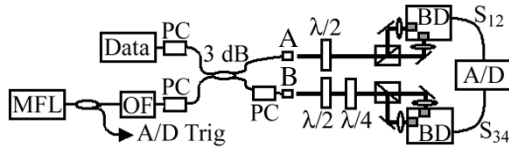


Fig. 1. Setup for linear optical sampling. MFL: mode-locked Erbium-doped fiber laser. OF: spectral filter. PC: polarization controller.  $\lambda/2$ : 1/2 wave plate.  $\lambda/4$ : 1/4 wave plate. BD: balanced detector. Microscope objectives are used at the outputs of the 3-dB coupler and for focusing to the balanced detectors.

(3) are squared and summed (in postdetection electronics or software), yielding the quantity

$$S(\tau) = 16 \left| \int \varepsilon_D(t) \varepsilon_S^*(t - \tau) dt \right|^2. \quad (4)$$

Therefore, we obtain the modulus square of the field cross correlation between the sampling pulse and the data pulse, in which the strong phase dependence of each single quadrature is removed.

Linear optical sampling is distinct from other sampling methods because it involves a field sampling rather than intensity sampling [6], [7]. Nonlinear optical sampling yields the quantity  $\int |E_D(t)|^2 |E_S(t - \tau)|^2 dt$ , which for a short sampling pulse is proportional to the data intensity  $I_D(\tau)$ . In contrast, some phase information is preserved in the signal generated by field sampling. Writing (4) in the Fourier domain

$$S(\tau) \approx \left| \int \tilde{\varepsilon}_D(\omega) \tilde{\varepsilon}_S^*(\omega) \exp(i\omega\tau) d\omega \right|^2 \quad (5)$$

we see that field sampling is sensitive to the relative spectral phase difference between the two pulses. If the spectral representation of the sampling pulse is reasonably constant in amplitude and phase across the spectral support of the data signal, the sampling field  $\tilde{\varepsilon}_S(\omega)$  can be taken out of the Fourier transform and the signal is  $S(\tau) \sim I_D(\tau)$ , which is equivalent to nonlinear sampling result with infinite resolution. From (5), it is clear that only the portion of the sampling pulse spectrum that overlaps with the data spectrum participates in the linear sampling, as expected for a homodyne measurement [10].

In our experiment, we use common-path polarization interferometers. The sampling pulses are generated from a Calmar Optcom mode-locked fiber laser running at a repetition rate close to 10 MHz. The offset between that frequency and the frequency of the data sources under test naturally scans the delay between the sampling and the data pulses, as in nonlinear optical sampling. The temporal axis of the measured eye diagrams was set by matching the period of the measured samples to the known period of the data. Because of the wide optical spectrum of the sampling laser, we have spectrally filtered our sampling pulses in order to match the bandwidth of the data signal. A 0.3-nm-wide spectral filter was used for measurements at 10 Gb/s while a 1-nm-wide filter was used at 40 and 80 Gb/s. The filters were tuned in each case to provide the best spectral overlap between the data and sampling fields. Following Fig. 1, the data and sampling pulses are initially polarized, respectively, along  $\hat{x}$  and  $\hat{y}$ . They are combined in a fiber-optic 50/50 coupler, with the two outputs then coupled to free space. Following

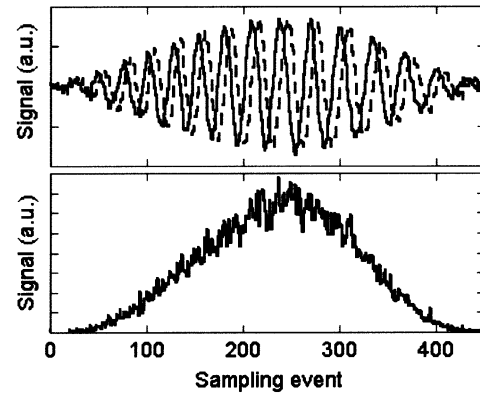


Fig. 2. Measured quadratures (continuous and dashed line) on a 10-Gb/s pulse train (upper plot) and waveform obtained by postdetection squaring and summing of the two quadratures (lower plot). Regular fringes are observed for measurement times on the order of the coherence times of the two sources (measurement time here was 50  $\mu$ s). As expected, the relative phase of the fringes in the two quadratures is  $\pi/2$ . Note that for data-encoded sources, no regular pattern on the quadratures is observed, as sampling events randomly occur for zeros and ones.

output A, after propagation through a half-wave plate, the data pulse is polarized along  $\hat{x} + \hat{y}$  while the sampling pulse is polarized along  $\hat{x} - \hat{y}$ . A polarizing beam splitter with its axis along  $\hat{x}$  and  $\hat{y}$  is then used to send independently  $(1/2)(E_S + E_D)$  and  $(1/2)(E_S - E_D)$  onto the two detectors of a New Focus 1617-AC balanced photodetector. This allows the measurement of the quadrature defined by (2). Output B of the coupler is identical, except that an additional quarter wave plate is set in order to induce a  $\pi/2$  phase shift between the sampling and the data pulse. The fields incident on the detectors of the other balanced detector in that arm are then  $(1/2)(E_S + iE_D)$  and  $(1/2)(E_S - iE_D)$ , and this allows the measurement of the quadrature defined by (3). The output current of each balanced photodetector is sent to a 1250 Gage Compuscope analog-to-digital (A/D) converting board. The acquisition is synchronized to the sampling pulses by means of a photodiode on which a small fraction of the sampling pulse is sent. After conversion, the two quadratures are numerically squared and summed in order to get the quantity described by (4). Fig. 2 displays an example of the two measured quadratures and the final signal obtained for a periodic train of pulses at 10 Gb/s.

We have first measured eye diagrams on a 10-Gb/s return-to-zero (RZ) data stream generated by carving of the light from a distributed feedback laser with a Mach-Zehnder LiNbO<sub>3</sub> modulator and data modulation with another identical modulator. The average power of the filtered sampling pulse is  $-18$  dBm. Open eye diagrams could be measured at data average powers down to  $-20$  dBm. This represents a sensitivity better than  $10^{-3}$  mW<sup>2</sup>, calculated as the product of the sampling average power and data peak power. Eye diagrams measured at  $-10$  and  $-20$  dBm are plotted in Fig. 3. The average power of our sampling pulses is very low compared to previous works on nonlinear optical sampling. Note, however, that the definition of the sensitivity takes this feature into account.

We have performed eye-diagram measurements at 40 and 80 Gb/s. The 40-Gb/s RZ signal is generated with four data-encoded time-multiplexed 10-Gb/s nonreturn-to-zero

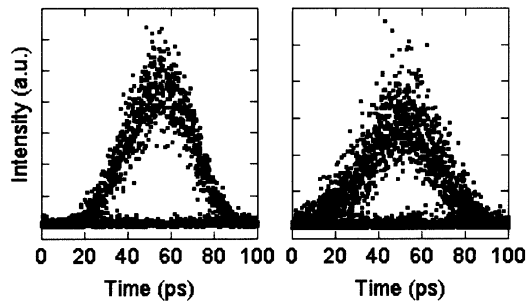


Fig. 3. The 10-Gb/s eye diagrams at a data average power of  $-10$  (left) and  $-20$  dBm (right). The average power of the sampling laser is  $-18$  dBm.

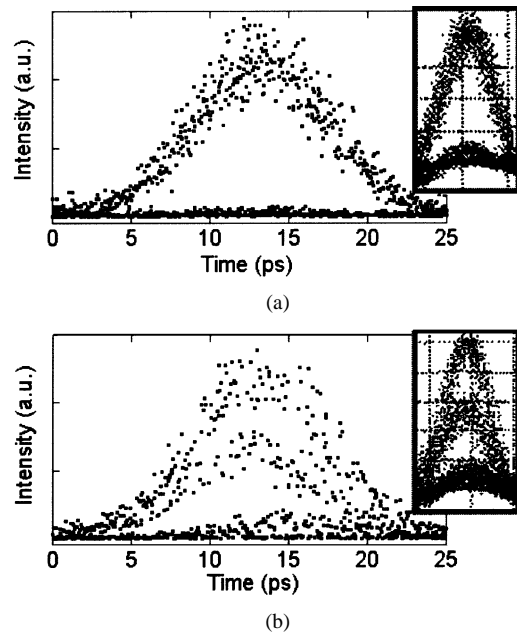


Fig. 4. (a) Eye diagrams at 40 Gb/s for an optimized and (b) misaligned carver-data modulator setup. In each case, the upper right inset is the readout from a 50-GHz sampling scope. The average power of the data is  $-1$  dBm and the average power of the sampling laser is  $-20$  dBm.

electrical signals and carved by an electroabsorption modulator. The 80-Gb/s data stream is generated by compression of the 40-Gb/s data stream and optical multiplexing. The average power of the sampling pulses was  $-20$  dBm at both bit rates. Open eye diagrams could be measured at data average power as low as  $-10$  dBm. Measured eye diagrams at 40 Gb/s at an average power of  $-1$  dBm are plotted on Fig. 4. The eye for an optimized system is plotted in Fig. 4(a). The inset is a readout from a fast photodiode and 50-GHz electronic sampling scope. The delay between the pulse carver and the data modulator was then modified in order to deteriorate the eye diagram [Fig. 4(b)]. These comparisons demonstrate that, although field sampling does not necessarily operate as intensity sampling, good agreement is obtained. Measured eye diagrams at 80 Gb/s for average data powers of  $-2$  and  $-11$  dBm are plotted in Fig. 5. At that bit rate, no information from the electronic sampling scope could be obtained.

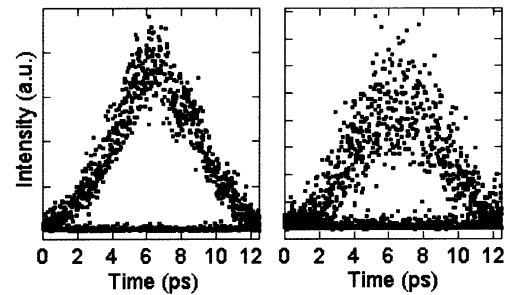


Fig. 5. The 80-Gb/s eye diagrams at a data average power of  $-2$  (left) and  $-11$  dBm (right). The average power of the sampling laser is  $-20$  dBm.

In conclusion, linear optical sampling has been used to measure eye diagrams at high bit rates. The eye diagram is reconstructed from the two quadratures of the interference between the data stream and a sampling source. Because this diagnostic uses only linear optics and square-law integrating detectors, it displays unprecedented sensitivity, 1000 times better than nonlinear optical sampling techniques. As with other optical sampling techniques, the time resolution can be adapted by a proper choice of the bandwidth of the sampling pulse for extension to higher bit rates. The high sensitivity and passive linear optical setup promise to enable a new class of monitoring applications.

#### REFERENCES

- [1] M. H. Chou, I. Brener, G. Lenz, R. Scotti, E. E. Chaban, J. Shmulyovich, D. Philen, S. Kosinski, K. R. Parameswaran, and M. M. Fejer, "Efficient wideband and tunable midspan spectral inverter using cascaded nonlinearities in LiNbO<sub>3</sub> waveguides," *IEEE Photon. Technol. Lett.*, vol. 12, pp. 82–84, Jan. 2000.
- [2] S. Diez, R. Ludwig, C. Schmidt, U. Feiste, and H. G. Weber, "160-Gb/s optical sampling by gain-transparent four-wave mixing in a semiconductor optical amplifier," *IEEE Photon. Technol. Lett.*, vol. 11, pp. 1402–1404, Nov. 1999.
- [3] S. Kawanishi, T. Yamamoto, M. Nakawawa, and M. M. Fejer, "High sensitivity waveform measurement with optical sampling using quasiphasematched mixing in LiNbO<sub>3</sub> waveguide," *Electron. Lett.*, vol. 37, pp. 844–846, 2001.
- [4] J. Li, J. Hansryd, P. O. Hedekvist, P. A. Andrekson, and S. N. Knudsen, "300 Gb/s eye-diagram measurement by optical sampling using fiber-based parametric amplification," *IEEE Photon. Technol. Lett.*, vol. 13, pp. 987–989, Sept. 2001.
- [5] S. Nogiwa, H. Ohta, Y. Kawaguchi, and Y. Endo, "Improvement of sensitivity in optical sampling system," *Electron. Lett.*, vol. 35, pp. 917–918, 1999.
- [6] D. T. Smithey, M. Beck, M. G. Raymer, and A. Faridani, "Measurement of the Wigner distribution and the density matrix of a light mode using optical homodyne tomography: Application to squeezed states and the vacuum," *Phys. Rev. Lett.*, vol. 70, pp. 1244–1247, 1993.
- [7] M. Munroe, D. Boggavarapu, M. E. Anderson, and M. G. Raymer, "Photon-number statistics from the phase-averaged quadrature-field distribution: Theory and ultrafast measurement," *Phys. Rev. A, Rapid Commun.*, vol. 52, pp. R924–R927, 1995.
- [8] K. Kikuchi, "Optical sampling system at 1.5 micron using two-photon absorption in Si avalanche photodiode," *Electron. Lett.*, vol. 34, pp. 1354–1355, 1998.
- [9] B. C. Thomsen, L. P. Barry, J. M. Dudley, and J. D. Harvey, "Ultra-sensitive all-optical sampling at 1.5 micron using waveguide two-photon absorption," *Electron. Lett.*, vol. 35, pp. 1483–1484, 1999.
- [10] M. E. Anderson, M. Munroe, U. Leonhardt, D. Boggavarapu, D. F. McAlister, and M. G. Raymer, "Ultrafast balanced-homodyne chronocyclic spectrometer," in *Proc. Generation, Amplification, and Measurement Ultrafast Laser Pulses III*, 1996, pp. 142–151.